Local discontinuous Galerkin method for incompressible miscible displacement problem in porous media *

Hui Guo†, Fan Yu‡, Yang Yang§

Abstract: In this paper, we develop local discontinuous Galerkin method for the two-dimensional coupled system of incompressible miscible displacement problem. Optimal error estimates in $L^\infty(0,T;L^2)$ for concentration c, $L^2(0,T;L^2)$ for ∇c and $L^\infty(0,T;L^2)$ for velocity $\mathbf{u}$ are derived. The main techniques in the analysis include the treatment of the inter-element jump terms which arise from the discontinuous nature of the numerical method, the nonlinearity, and the coupling of the models. The main difficulty is how to treat the inter-element discontinuities of two independent solution variables (one from the flow equation and the other from the transport equation) at cell interfaces. Numerical experiments are shown to demonstrate the theoretical results.

Keywords: incompressible miscible displacement problem; local discontinuous Galerkin method; error estimate

AMS(2000) Subject Classifications: 65M15, 65M60.

1 Introduction

Numerical modeling of miscible displacement in porous media is important and interesting in oil recovery and enviromental pollution problem. The miscible displacement problem is described by a coupled system of nonlinear partial differential equations. The need for accurate solutions to the coupled equations challenges numerical analysts to design new methods. Popular methods for solving miscible displacement in porous media numerically employ nonconforming discrete spaces containing discontinuous functions and introduce special numerical techniques to control jumps of numerical approximations as well as the nonlinearality of the convection term, known as discontinuous Galerkin (DG) methods.

The DG method gained even greater popularity recently for good stability, high order accuracy, and flexibility on h-p adaptivity and on complex geometry. But, it is difficult to

*Supported by National Natural Science Foundation of China(11571367) and the Fundamental Research Funds for the Central Universities.

†College of Science, China University of Petroleum, Qingdao 266580, China. E-mail: sdugh@163.com

‡College of Science, China University of Petroleum, Qingdao 266580, China. E-mail: yufanliyun@163.com

§Michigan Technological University, Houghton, MI 49931, USA. E-mail:yyang7@mtu.edu

apply the DG method directly to the equations with higher order derivatives. The idea of the local discontinuous Galerkin (LDG) method is to rewrite the equations with higher order derivatives into a first order system, then apply the DG method to the system. As an extension of DG schemes for hyperbolic conservation laws, this scheme shares the advantages of the DG methods. Besides, a key advantage of this scheme is the local solvability, that is, the auxiliary variables approximating the derivatives of the solution can be locally eliminated. The first LDG method was constructed by Cockburn and Shu in [9] for solving nonlinear convection diffusion equations containing second order spatial derivatives. Their work was motivated by the successful numerical experiments of Bassi and Rebay [3] for the compressible Navier-Stokes equations. The methods were further developed in [37, 35, 36] for solving many nonlinear wave equations with higher order derivatives.

In a previous work, Douglas et. al. [11, 12] presented the mixed finite element method for miscible displacement problem. Subsequently, there were plenty of significant works with conforming methods have been studied [16, 14, 25, 33]. Later, many numerical techniques have been introduced to obtain better approximations, such as numerical methods of characteristics, e.g., [15, 40], Eulerian-Lagrangian localized adjoint methods [29], upstream weighting and mixed finite elements [21] and mass-conservative characteristic finite element method [23]. Besides, in [6], the authors applied the DDFV scheme to the problem and studied convergence of the scheme. In [1], the authors introduced the mixed finite element and finite volume methods. Later, Kumar [22] discussed a mixed and discontinuous finite volume method for incompressible miscible displacement problems, another related work can be found in [38]. Moreover, the DG methods for miscible displacement have been investigated by numerical experiments and was reported to exhibit good numerical performance [34, 2, 24]. In [27], [28], [10], primal semi-discrete discontinuous Galerkin methods with interior penalty are proposed to solve the coupled system of flow and reactive transport in porous media. For a more detailed early works in the literature, we refer to [17].

In our previous work [19], we have used the LDG method to discretize the transport equation. For the flow equation, we still used the continuous mixed finite element methods to avoid having discontinuities of two independent solution variables at cell interfaces. In this paper, we continue our work for developing LDG method for flow and transport in two space dimensions. Different from [19], the flow equation is also discretized by the LDG method. Although there have been many theoretical analyses of the LDG method, the one for incompressible miscible displacement problem, by a unified LDG method to both for the flow equation and transport equation, still seems to be unavailable. The main difficulty is how to treat the inter-element discontinuities of two independent solution

variables (one from the flow equation and the other from the transport equation) at cell interfaces. More precisely, in this problem, the approximations of $\mathbf{u}$ in the convection term in (2.1) are discontinuous across the cell interfaces and it is difficult to obtain error estimates if we analyze the convection and diffusion terms separately. To explain this point, let us consider the following hyperbolic equation

$$u_t + (a(x)u)_x = 0,$$

where $a(x)$ is discontinuous at $x = x_0$. In [18, 20], the authors studied such a problem and defined

$$Q = \frac{a(x_0 + b) - a(x_0)}{b}.$$

If Q is bounded from below for all b, then the solution exists, but may not be unique. If Q is bounded from above for all b, we can guarantee the uniqueness, but the solution may not exist. In our problem, even though the velocity can be continuous, the DG approximations of the velocity are discontinuous across the cell interfaces, leading to ill-posed problems. To obtain the error estimates, we need the help of the diffusion term in the equation. Recently, Wang et al. [30, 31, 32] obtained optimal error estimates of the LDG methods with implicit-explicit time marching for linear and nonlinear convection-diffusion problems. The key idea is to explore an important relationship between the gradient and interface jump of the numerical solution with the approximation of auxiliary variable for the gradient in the LDG methods, which is stated in Lemma 3.4. We will use this key lemma to obtain optimal error estimates in $L^\infty(0, T; L^2)$ for concentration c, in $L^2(0, T; L^2)$ for $\mathbf{s} = -\nabla c$ and $L^\infty(0, T; L^2)$ for velocity $\mathbf{u}$. Here we should mention the difference between our LDG method and the DG methods in [28], where the interior penalty method was developed and optimal error estimates in $L^2(0, T; H^1)$ norm for concentration c were derived. In our proof, induction hypothesis is used as a tool, instead of the cut-off operator introduced in [28]. This can avoid the difficulty in how to choose the sufficiently large positive constant M, and the possibility of infinite times of loops for extreme cases.

The paper is organized as follows. In Section 2, we present some preliminaries, including the basic notations and norms we use throughout the paper, the LDG spatial discretization as well as the error equations. Section 3 is the main body of the paper where we present the projections and some essential properties of the finite element spaces, error equations and the details of the optimal error estimates for incompressible miscible displacement problem. Then numerical results are given to demonstrate the accuracy and capability of the method in Section 4. We will end in Section 5 with some concluding remarks.

2 Incompressible miscible displacement problem

In this section, we give the analysis for incompressible miscible displacement problem. Detailed discussion on physical theories of miscible displacement in porous media can be found in [4, 13]. Let Ω be a bounded domain. The classical equations governing the incompressible miscible displacement in porous media in two space dimensions are as follows:

$$\begin{aligned} &\nabla \cdot \mathbf{u} = q, && (x,y) \in \Omega, 0 < t \leq T, \\ &\mathbf{u} = \tfrac{-\kappa(x,y)}{\mu(c)} \nabla p, && (x,y) \in \Omega, 0 < t \leq T, \\ &\phi \tfrac{\partial c}{\partial t} + \nabla \cdot (\mathbf{u}c) = \nabla \cdot (\mathbf{D}(\mathbf{u}) \nabla c) + \tilde{c}q, && (x,y) \in \Omega, 0 < t \leq T, \end{aligned} \tag{2.1}$$

where the dependent variables p, $\mathbf{u}$ and c are the pressure in the fluid mixture, the Darcy velocity of the mixture (volume flowing across a unit cross-section per unit time), and the concentration of interested species measured in amount of species per unit volume of the fluid mixture, respectively. ϕ and κ are the porosity and the permeability of the rock, respectively. μ is the concentration-dependent viscosity. q is the external volumetric flow rate, and $\tilde{c}$ is the concentration of the fluid in the external flow. $\tilde{c}$ must be specified at points at which injection ($q > 0$) takes place, and is assumed to be equal to c at production points ($q < 0$). The diffusion coefficient $\mathbf{D}$ arises from two aspects: molecular diffusion, which is rather small for field-scale problems, and dispersion, which is velocity-dependent, in the petroleum engineering literature. Its form is

$$\mathbf{D} = \phi(x)(d_{mol}\mathbf{I} + d_{long}|\mathbf{u}|\mathbf{E} + d_{tran}|\mathbf{u}|\mathbf{E}^{\perp}), \tag{2.2}$$

where $\mathbf{E}$, a 2×2 matrix, represents the orthogonal projection along the velocity vector and is given by

$$\mathbf{E} = (e_{ij}(\mathbf{u})) = \left(\frac{u_i u_j}{|\mathbf{u}|^2} \right), \quad \mathbf{u} = (u_1, u_2),$$

and $\mathbf{E}^{\perp} = \mathbf{I} - \mathbf{E}$ is the orthogonal complement. The diffusion coefficient d_{long} measures the dispersion in the direction of the flow and d_{tran} shows that transverse to the flow. In this paper, the tensor matrix $\mathbf{D}(\mathbf{u})$ is assumed to be positive definite. Moreover, the pressure is uniquely determined up to a constant, thus we assume $\int_{\Omega} p dx dy = 0$. For simplicity, we only consider periodic boundary conditions. However, this assumption is not essential, the proof for homogeneous Neumann boundary conditions can be obtained with some minor changes. In this problem, the initial concentration is given as

$$c(x, y, 0) = c_0(x, y), \quad (x, y) \in \Omega.$$

Finally, we make the following hypotheses (H) for (2.1).

1. $0 < \kappa_* \leq \kappa(x, y) \leq \kappa^*$, $0 < \mu_* \leq \mu(c) \leq \mu^*$, $0 < \phi_* \leq \phi(x, y) \leq \phi^*$ and $|q| \leq C$,

2. $\mu(c)$ is uniformly Lipschtiz continuous with respect to c.

3. $\mathbf{D}(\mathbf{u})$ is positive definite, i.e. there exists $D_* > 0$, such that for any $\mathbf{v} \in R^2$, $D_*\|\mathbf{v}\|^2 \leq \mathbf{v}^T\mathbf{D}(\mathbf{u})\mathbf{v}$.

4. $\mathbf{u}, \nabla \cdot \mathbf{u}, c, \nabla c, \mathbf{D}(\mathbf{u})$ are uniformly bounded in R^2.

Besides the above, $\mathbf{D}(\mathbf{u})$ also satisfies the following property [27]

Lemma 2.1 $\mathbf{D}(\mathbf{u})$ *is uniformly Lipschtiz continuous with respect to* $\mathbf{u}$.

2.1 Basic notations

In this section, we demonstrate the notations that will be used throughout the paper. Let $0 = x_{\frac{1}{2}} < \cdots < x_{N_x+\frac{1}{2}} = 1$ and $0 = y_{\frac{1}{2}} < \cdots < y_{N_y+\frac{1}{2}} = 1$ be the grid points in the x and y directions, respectively. Define $I_i = (x_{i-\frac{1}{2}}, x_{i+\frac{1}{2}})$ and $J_j = (y_{j-\frac{1}{2}}, y_{j+\frac{1}{2}})$. Let $K_{ij} = I_i \times J_j$, $i = 1, \cdots, N_x,\ j = 1, \cdots, N_y$, be a partition of Ω and denote $\Omega_h = \{K_{ij}\}$. For simplicity, if not otherwise stated, we always use K to denote the cell. The mesh sizes in the x and y directions are given as $\Delta x_i = x_{i+\frac{1}{2}} - x_{i-\frac{1}{2}}$ and $\Delta y_j = y_{j+\frac{1}{2}} - y_{j-\frac{1}{2}}$, respectively and denote $h = \max(\max_i \Delta x_i, \max_j \Delta y_j)$. Moreover, we assume the partition is quasi-uniform. The finite element space is chosen as

$$W_h^k = \{z : z|_K \in Q^k(K), \forall K \in \Omega_h\},$$

where $Q^k(K)$ denotes the space of tensor product of polynomials of degrees at most k in K. Note that functions in W_h^k are discontinuous across element interfaces. This is one of the main differences between the DG method and traditional finite element methods. We choose $\boldsymbol{\beta} = (1, 1)^T$ to be a fixes vector that is not parallel to any normals of the element interfaces. We denote Γ_h be the set of all element interfaces and $\Gamma_0 = \Gamma_h \backslash \partial\Omega$. Let $e \in \Gamma_0$ be an interior edge shared by elements K_ℓ and K_r, where $\boldsymbol{\beta} \cdot \mathbf{n}_\ell > 0$, and $\boldsymbol{\beta} \cdot \mathbf{n}_r < 0$, respectively, with $\mathbf{n}_\ell$ and $\mathbf{n}_r$ being the outward normal of K_ℓ and K_r, respectively. For any $z \in W_h^k$, we define $z^- = z|_{\partial K_\ell}$ and $z^+ = z|_{\partial K_r}$, respectively. The jump is given as $[z] = z^+ - z^-$. Moreover, for $\mathbf{s} \in \mathbf{W}_h^k = W_h^k \times W_h^k$, we define $\mathbf{s}^+$ and $\mathbf{s}^-$ and $[\mathbf{s}]$ analogously. Further more, we define $\partial\Omega_- = \{e \in \partial\Omega | \boldsymbol{\beta} \cdot \mathbf{n} < 0\}$, where $\mathbf{n}$ is the outer normal of e, and $\partial\Omega_+ = \partial\Omega \backslash \partial\Omega_-$. For any $e \in \partial\Omega_-$, there exists $K \in \Omega_h$ such that $e \in \partial K$, we define $z^+|_e = z|_{\partial K}$ and z^- on $\partial\Omega_+$ is defined analogously. For simplicity, given $e = \{x_{\frac{1}{2}}\} \times J_j \in \partial\Omega_-$, and $\tilde{e} = \{x_{N_x+\frac{1}{2}}\} \times J_j \in \partial\Omega_+$, by periodic boundary condition, we define

$$z^-|_e = z^-|_{\tilde{e}}, \quad \text{and} \quad z^+|_{\tilde{e}} = z^+|_e.$$

Similarly, given $e = I_i \times \{y_{\frac{1}{2}}\} \in \partial\Omega_-$, and $\tilde{e} = I_i \times \{y_{N_y+\frac{1}{2}}\} \in \partial\Omega_+$ we define

$$z^-|_e = z^-|_{\tilde{e}}, \quad \text{and} \quad z^+|_{\tilde{e}} = z^+|_e.$$

Throughout this paper, the symbol C is used as a generic constant which may appear differently at different occurrences.

2.2 Norms

In this subsection, we define several norms that will be used throughout the paper.

Denote $\|u\|_{0,K}$ to be the standard L^2 norm of u in cell K. For any natural number ℓ, we consider the norm of the Sobolev space $H^\ell(K)$, given as

$$\|u\|_{\ell,K} = \left\{ \sum_{0\le\alpha+\beta\le\ell} \left\| \frac{\partial^{\alpha+\beta} u}{\partial x^\alpha \partial y^\beta} \right\|_{0,K}^2 \right\}^{\frac{1}{2}}.$$

Moreover, we define the norms on the whole computational domain as

$$\|u\|_\ell = \left(\sum_{K\in\Omega_h} \|u\|_{\ell,K}^2 \right)^{\frac{1}{2}}.$$

For convenience, if we consider the standard L^2 norm, then the corresponding subscript will be omitted.

Let Γ_K be the edges of K, and we define

$$\|u\|_{\Gamma_K}^2 = \int_{\partial K} u^2 ds.$$

We also define

$$\|u\|_{\Gamma_h}^2 = \sum_{K\in\Omega_h} \|u\|_{\Gamma_K}^2.$$

Moreover, we denote the standard L^∞ norm of u in K as $\|u\|_{\infty,K}$, and the L^∞ norm on the whole computational domain is given as

$$\|u\|_\infty = \max_{K\in\Omega_h} \|u\|_{\infty,K}.$$

Finally, we define similar norms for vector $\mathbf{u} = (u_1, u_2)^T$ as

$$\|\mathbf{u}\|_{\ell,K}^2 = \|u_1\|_{\ell,K}^2 + \|u_2\|_{\ell,K}^2, \quad \|\mathbf{u}\|_{\Gamma_K}^2 = \|u_1\|_{\Gamma_K}^2 + \|u_2\|_{\Gamma_K}^2, \quad \|\mathbf{u}\|_{\infty,K} = \max\{\|u_1\|_{\infty,K}, \|u_2\|_{\infty,K}\}.$$

Similarly, the norms on the whole computational domain are given as

$$\|\mathbf{u}\|_\ell^2 = \sum_{K\in\Omega_h} \|\mathbf{u}\|_{\ell,K}^2, \quad \|\mathbf{u}\|_{\Gamma_h}^2 = \sum_{K\in\Omega_h} \|\mathbf{u}\|_{\Gamma_K}^2, \quad \|\mathbf{u}\|_\infty = \max_{K\in\Omega_h} \|\mathbf{u}\|_{\infty,K}.$$

2.3 LDG scheme and the main theorem

To construct the LDG scheme, we introduce some auxiliary variables to approximate the derivatives of the solution which further yields a first order system:

$$\phi\frac{\partial c}{\partial t}+\nabla\cdot(\mathbf{u}c)+\nabla\cdot\mathbf{z}=\tilde{c}q, \tag{2.3}$$
$$\mathbf{s}=-\nabla c, \tag{2.4}$$
$$\mathbf{z}=\mathbf{D}(\mathbf{u})\mathbf{s}, \tag{2.5}$$
$$A(c)\mathbf{u}=-\nabla p, \tag{2.6}$$
$$\nabla\cdot\mathbf{u}=q, \tag{2.7}$$

where $A(c)=A(x,y,c)=\frac{\mu(c)}{k(x,y)}$. We multiply (2.3)-(2.7) by test functions $v,\zeta\in W_h^k$, $\boldsymbol{\theta},\mathbf{w},\boldsymbol{\psi}\in\mathbf{W}_h^k$, respectively. Formally integrate by parts in K to get

$$\begin{aligned}
(\phi c_t,v)_K &= (\mathbf{u}c+\mathbf{z},\nabla v)_K-\langle(\mathbf{u}c+\mathbf{z})\cdot\boldsymbol{\nu}_K,v\rangle_{\partial K}+(\tilde{c}q,v)_K,\\
(\mathbf{s},\mathbf{w})_K &= (c,\nabla\cdot\mathbf{w})_K-\langle c,\mathbf{w}\cdot\boldsymbol{\nu}_K\rangle_{\partial K},\\
(\mathbf{z},\boldsymbol{\psi})_K &= (\mathbf{D}(\mathbf{u})\mathbf{s},\boldsymbol{\psi})_K,\\
(A(c)\mathbf{u},\boldsymbol{\theta})_K &= (p,\nabla\cdot\boldsymbol{\theta})_K-\langle p,\boldsymbol{\theta}\cdot\boldsymbol{\nu}_K\rangle_{\partial K},\\
-(\mathbf{u},\nabla\zeta)_K &= -\langle\mathbf{u}\cdot\boldsymbol{\nu}_K,\zeta\rangle_{\partial K}+(q,\zeta)_K.
\end{aligned}$$

where $(u,v)_K=\int_K uvdxdy$, $(\mathbf{u},\mathbf{v})_K=\int_K\mathbf{u}\cdot\mathbf{v}dxdy$, $\langle u,v\rangle_{\partial K}=\int_{\partial K}uvds$ and $\boldsymbol{\nu}_K$ is the outer normal of K. Replacing the exact solutions $c,\ p,\ \mathbf{s},\ \mathbf{z},\ \mathbf{u}$ in the above equations by their numerical approximations $c_h,\ p_h\in W_h^k$ and $\mathbf{s}_h,\ \mathbf{z}_h,\ \mathbf{u}_h\in\mathbf{W}_h^k$, respectively and using numerical fluxes at the cell interfaces to obtain the LDG scheme:

$$(\phi c_{ht},v)_K=\mathcal{L}_K^c(\mathbf{u}_h,c_h,v)+\mathcal{L}_K^d(\mathbf{z}_h,v)+(\tilde{c_h}q,v)_K, \tag{2.8}$$
$$(\mathbf{s}_h,\mathbf{w})_K=\mathcal{D}_K(c_h,\mathbf{w}), \tag{2.9}$$
$$(\mathbf{z}_h,\boldsymbol{\psi})_K=(\mathbf{D}(\mathbf{u}_h)\mathbf{s}_h,\boldsymbol{\psi})_K, \tag{2.10}$$
$$(A(c_h)\mathbf{u}_h,\boldsymbol{\theta})_K=\mathcal{D}_K(p_h,\boldsymbol{\theta}), \tag{2.11}$$
$$(q,\zeta)_K=-\mathcal{L}_K^d(\mathbf{u}_h,\zeta), \tag{2.12}$$

where

$$\mathcal{L}_K^d(\mathbf{s},v)=(\mathbf{s},\nabla v)_K-\langle\widehat{\mathbf{s}}\cdot\boldsymbol{\nu}_K,v\rangle_{\partial K}, \tag{2.13}$$
$$\mathcal{L}_K^c(\mathbf{s},c,v)=(\mathbf{s}c,\nabla v)_K-\langle\widehat{\mathbf{s}}\widehat{c}\cdot\boldsymbol{\nu}_K,v\rangle_{\partial K}, \tag{2.14}$$
$$\mathcal{D}_K(c,\mathbf{w})=(c,\nabla\cdot\mathbf{w})_K-\langle\widehat{c},\mathbf{w}\cdot\boldsymbol{\nu}_K\rangle_{\partial K}. \tag{2.15}$$

We use alternating fluxes for the diffusion term and take

$$\widehat{\mathbf{z}_h}=\mathbf{z}_h^-,\quad \widehat{c_h}=c_h^+,\quad \widehat{\mathbf{u}_h}=\mathbf{u}_h^-,\quad \widehat{p_h}=p_h^+.$$

For the convection term, we consider Lax-Friedrichs flux

$$\widehat{\mathbf{u}_h c_h} = \frac{1}{2}(\mathbf{u}_h^+ c_h^+ + \mathbf{u}_h^- c_h^- - \alpha \boldsymbol{\nu}_e (c_h^+ - c_h^-)),$$

where $\alpha > 0$ can be chosen as any constant and $\boldsymbol{\nu}_e$ is the normal of the $e \in \Gamma_0$ such that $\boldsymbol{\beta} \cdot \boldsymbol{\nu}_e > 0$. Moreover, we define

$$(u, v) = \sum_{K \in \Omega_h} (u, v)_K, \qquad (\mathbf{u}, \mathbf{v}) = \sum_{K \in \Omega_h} (\mathbf{u}, \mathbf{v})_K,$$

and

$$\mathcal{L}^d(\mathbf{s}, v) = \sum_{K \in \Omega_h} \mathcal{L}_K^d(\mathbf{s}, v), \qquad \mathcal{L}^c(\mathbf{s}, c, v) = \sum_{K \in \Omega_h} \mathcal{L}_K^c(\mathbf{s}, c, v), \qquad \mathcal{D}(c, \mathbf{w}) = \sum_{K \in \Omega_h} \mathcal{D}_K(c, \mathbf{w}).$$

It is easy to check the following identity by integration by parts on each cell: for any functions v and $\mathbf{w}$,

$$\mathcal{L}^d(\mathbf{w}, v) + \mathcal{D}(v, \mathbf{w}) = 0. \tag{2.16}$$

The initial solution is taken as the L^2-projection (see (3.1) for the definition). Now we state the main theorem.

Theorem 2.1 *Let $c \in H^{k+3}, \mathbf{s} \in (H^{k+2})^2, \mathbf{u} \in (H^{k+1})^2$ be the exact solutions of the problem* (2.3)-(2.7)*, and let $c_h, \mathbf{s}_h, \mathbf{u}_h$ be the numerical solution of the semi-discrete LDG scheme* (2.8)-(2.12)*. If the finite element space is the piecewise polynomials of degree $k \geq 1$ and h is sufficiently small, then we have the error estimate*

$$\|c - c_h\|_{L^\infty(0,T;L^2)} + \|\mathbf{s} - \mathbf{s}_h\|_{L^2(0,T;L^2)} + \|\mathbf{u} - \mathbf{u}_h\|_{L^\infty(0,T;L^2)} \leq C h^{k+1}, \tag{2.17}$$

where the constant C is independent of the mesh parameter h.

Remark 2.1 *In this paper, we consider Lax-Friedrichs flux for convection term only. However, the result in Theorem 2.1 is also valid for general fluxes that are consistent and Lipschitz continuous.*

3 The proof of the main theorem

In this section, we proceed to the proof of Theorem 2.1. We first introduce several projections and present some auxiliary results. Subsequently, we make an a priori error estimate which provides the boundedness of the numerical approximations. Then we construct the error equations which further yield two main energy inequalities and complete the proof of (2.17). Finally, we verify the a priori error estimate at the end of this section.

3.1 Projections and interpolation properties

In this section, we will demonstrate the projections and several useful lemmas. Let us start with the classical inverse properties [7].

Lemma 3.1 *Assuming $u \in W_h^k$, there exists a positive constant C independent of h and u such that*

$$h\|u\|_{\infty,K} + h^{1/2}\|u\|_{\Gamma_K} \leq C\|u\|_K.$$

We will use several special projections in this paper. Firstly, we define P^+ into W_h^k which is, for each cell K

$$(P^+u - u, v)_K = 0, \forall v \in Q^{k-1}(K), \int_{J_j} (P^+u - u)(x_{i-\frac{1}{2}}, y)v(y)dy = 0, \forall v \in P^{k-1}(J_j),$$
$$(P^+u - u)(x_{i-\frac{1}{2}}, y_{j-\frac{1}{2}}) = 0, \int_{I_i} (P^+u - u)(x, y_{j-\frac{1}{2}})v(x)dx = 0, \forall v \in P^{k-1}(I_i).$$

where P^k denotes the polynomials of degree k. Moreover, we also define Π^x and Π^y into W_h^k which are, for each cell K,

$$(\Pi^x u - u, v_x)_K = 0, \forall v \in Q^k(K), \int_{J_j} (\Pi^x u - u)(x_{i+\frac{1}{2}}, y)v(y)dy = 0, \forall v \in P^k(J_j),$$
$$(\Pi^y u - u, v_y)_K = 0, \forall v \in Q^k(K), \int_{I_i} (\Pi^y u - u)(x, y_{j+\frac{1}{2}})v(x)dx = 0, \forall v \in P^k(I_i),$$

as well as a two-dimensional projection $\mathbf{\Pi} = \Pi^x \otimes \Pi^y$. Finally, we also use the L^2-projection P_k into W_h^k which is, for each cell K

$$(P_k u - u, v)_K = 0, \forall v \in Q^k(K), \tag{3.1}$$

and its two dimensional version $\mathbf{P}_k = P_k \otimes P_k$. For the special projections mentioned above, we give the following lemma by the standard approximation theory [7].

Lemma 3.2 *Suppose $w \in H^{k+1}(\Omega)$, then for any projection P_h, which is either P^+, Π^x, Π^y or P_k, we have*

$$\|w - P_h w\| + h^{1/2}\|w - P_h w\|_{\Gamma_h} \leq Ch^{k+1}.$$

Moreover, the projection P^+ on the Cartesian meshes has the following superconvergence property (see [5], Lemma 3.6).

Lemma 3.3 *Suppose $w \in H^{k+2}(\Omega)$, then for any $\boldsymbol{\rho} \in \mathbf{W}_h$ we have*

$$|\mathcal{D}(w - P^+w, \boldsymbol{\rho})| \leq Ch^{k+1}\|w\|_{k+2}\|\boldsymbol{\rho}\|. \tag{3.2}$$

In this paper, we use e to denote the error between the exact and numerical solutions, i.e. $e_c = c - c_h,\ e_p = p - p_h\ \mathbf{e}_u = \mathbf{u} - \mathbf{u}_h,\ \mathbf{e}_s = \mathbf{s} - \mathbf{s}_h,\ \mathbf{e}_z = \mathbf{z} - \mathbf{z}_h$. As the general treatment of the finite element methods, we split the errors into two terms as

$$\begin{array}{lll} e_c = \eta_c - \xi_c, & \eta_c = c - P^+c, & \xi_c = c_h - P^+c, \\ e_p = \eta_p - \xi_p, & \eta_p = p - P^+p, & \xi_p = p_h - P^+p, \\ \mathbf{e}_u = \boldsymbol{\eta}_u - \boldsymbol{\xi}_u, & \boldsymbol{\eta}_u = \mathbf{u} - \boldsymbol{\Pi}\mathbf{u}, & \boldsymbol{\xi}_u = \mathbf{u}_h - \boldsymbol{\Pi}\mathbf{u}, \\ \mathbf{e}_s = \boldsymbol{\eta}_s - \boldsymbol{\xi}_s, & \boldsymbol{\eta}_s = \mathbf{s} - \mathbf{P}_k\mathbf{s}, & \boldsymbol{\xi}_s = \mathbf{s}_h - \mathbf{P}_k\mathbf{s}, \\ \mathbf{e}_z = \boldsymbol{\eta}_z - \boldsymbol{\xi}_z, & \boldsymbol{\eta}_z = \mathbf{z} - \boldsymbol{\Pi}\mathbf{z}, & \boldsymbol{\xi}_z = \mathbf{z}_h - \boldsymbol{\Pi}\mathbf{z}. \end{array}$$

Based on the above, it is easy to see that

$$\mathcal{L}^d(\boldsymbol{\eta}_u, v) = \mathcal{L}^d(\boldsymbol{\eta}_z, v) = 0,\ \forall v \in W_h^k. \tag{3.3}$$

Following [39, 30, 31, 32] with some minor changes, we have the following lemma

Lemma 3.4 *Suppose ξ_c and $\boldsymbol{\xi}_s$ are defined above, we have*

$$\|\nabla \xi_c\| \le C(\|\boldsymbol{\xi}_s\| + h^{k+1}), \qquad h^{-\frac{1}{2}}\|[\xi_c]\|_{\Gamma_h} \le C(\|\boldsymbol{\xi}_s\| + h^{k+1}).$$

3.2 A priori error estimate

In this subsection, we would like to make an a priori error estimate

$$\|c - c_h\| + \|\mathbf{u} - \mathbf{u}_h\| \le h, \tag{3.4}$$

which further implies

$$\|c_h\|_\infty + \|\mathbf{u}_h\|_\infty \le C \tag{3.5}$$

by hypotheses 4. Then by the Lemma 2.1 and hypothesis 4, we have

$$|||\mathbf{D}(\mathbf{u}_h)||| \le C, \tag{3.6}$$

where $|||\mathbf{D}||| = \|\max\{|d_{11}|, |d_{12}|, |d_{21}|, |d_{22}|\}\|_\infty$ with $\mathbf{D} = \{d_{ij}\}_{2\times 2}$. This idea has been used to obtain error estimates for nonlinear hyperbolic equations [41, 42]. With this assumption, we can proceed to the main proof of the theorem.

3.3 Error equations

In this section, we proceed to construct the error equations. From (2.8)-(2.12), we have the following error equations

$$(\phi e_{ct}, v) = \mathcal{L}^c(\mathbf{u}, c, v) - \mathcal{L}^c(\mathbf{u}_h, c_h, v) + \mathcal{L}^d(\mathbf{e}_z, v) + (\tilde{e_c}q, v), \tag{3.7}$$

$$(\mathbf{e}_s, \mathbf{w}) = \mathcal{D}(e_c, \mathbf{w}), \tag{3.8}$$

$$(\mathbf{e}_z, \boldsymbol{\psi}) = (\mathbf{D}(\mathbf{u})\mathbf{s} - \mathbf{D}(\mathbf{u}_h)\mathbf{s}_h, \boldsymbol{\psi}), \tag{3.9}$$

$$((A(c)\mathbf{u} - A(c_h)\mathbf{u}_h), \boldsymbol{\theta}) = \mathcal{D}(e_p, \boldsymbol{\theta}), \tag{3.10}$$

$$\mathcal{L}^d(\mathbf{e}_u, \zeta) = 0, \tag{3.11}$$

$\forall v, \zeta \in W_h^k, \boldsymbol{\theta}, \mathbf{w}, \boldsymbol{\psi} \in \mathbf{W}_h^k$, where

$$\tilde{e_c} = \begin{cases} 0, & q > 0, \\ e_c, & q < 0. \end{cases}$$

3.4 The first energy inequality

We start from an easier case. Take $\boldsymbol{\theta} = \boldsymbol{\xi}_u$ and $\zeta = \xi_p$ in (3.10) and (3.11), respectively and use (2.16) and (3.3) to obtain

$$(A(c)\boldsymbol{\xi}_u, \boldsymbol{\xi}_u) = T_1 + T_2 - T_3, \tag{3.12}$$

where

$$\begin{aligned} T_1 &= (A(c)\boldsymbol{\eta}_u, \boldsymbol{\xi}_u), \\ T_2 &= ((A(c) - A(c_h))\mathbf{u_h}, \boldsymbol{\xi}_u), \\ T_3 &= \mathcal{D}(\eta_p, \boldsymbol{\xi}_u). \end{aligned}$$

Now, we estimate $T_i's$ term by term. Using Lemma 3.2 and Schwarz inequality, we can get

$$T_1 \leq C\|\boldsymbol{\eta}_u\|\|\boldsymbol{\xi}_u\| \leq Ch^{k+1}\|\boldsymbol{\xi}_u\|, \tag{3.13}$$

Here, we use the hypotheses 1 then $A(c) \leq \mu^*/\kappa_*$. The estimate of T_2 is slightly complicated,

$$\begin{aligned} T_2 &\leq C\|(A(c) - A(c_h))\|\|\boldsymbol{\xi}_u\| \\ &\leq C\|c - c_h\|\|\boldsymbol{\xi}_u\| \\ &\leq C\left(h^{k+1} + \|\xi_c\|\right)\|\boldsymbol{\xi}_u\|, \end{aligned} \tag{3.14}$$

where in the first step we use Schwarz inequality and hypothesis 4, the second step follows from hypothesis 2, and the last step requires Lemma 3.2. For T_3, we use Lemma 3.3 to obtain

$$T_3 \leq Ch^{k+1}\|p\|_{k+2}\|\boldsymbol{\xi}_u\|. \tag{3.15}$$

Substituting (3.13), (3.14) and (3.15) into (3.12), we have the estimate

$$\|\sqrt{A(c)}\boldsymbol{\xi}_u\|^2 \leq C\left(h^{k+1} + \|\xi_c\|\right)\|\boldsymbol{\xi}_u\|.$$

which further yield the first energy estimate

$$\|\boldsymbol{\xi}_u\| \leq Ch^{k+1} + C\|\xi_c\|, \tag{3.16}$$

by hypothesis 1.

3.5 The second energy inequality

Taking the test functions $v = \xi_c$, $\mathbf{w} = \boldsymbol{\xi}_z$, and $\boldsymbol{\psi} = -\boldsymbol{\xi}_s$ in (3.7), (3.8) and (3.9), respectively, and using (2.16) and (3.3) we obtain

$$(\phi\frac{\partial \xi_c}{\partial t}, \xi_c) + (\mathbf{D}(\mathbf{u}_h)\boldsymbol{\xi}_s, \boldsymbol{\xi}_s) = R_1 + R_2 - R_3 - R_4 + R_5, \tag{3.17}$$

where

$$\begin{aligned}
R_1 &= (\phi\frac{\partial \eta_c}{\partial t}, \xi_c) + (\mathbf{D}(\mathbf{u}_h)\boldsymbol{\eta}_s, \boldsymbol{\xi}_s)\,,\\
R_2 &= ((\mathbf{D}(\mathbf{u}) - \mathbf{D}(\mathbf{u}_h))\mathbf{s}, \boldsymbol{\xi}_s)\,,\\
R_3 &= (\mathbf{u}c - \mathbf{u}_h c_h, \nabla\xi_c) - \sum_{e\in\Gamma_e}\langle(\mathbf{u}c - \widehat{\mathbf{u}_h c_h})\cdot\boldsymbol{\nu}_e, [\xi_c]\rangle_e,\\
R_4 &= \mathcal{D}(\eta_c, \boldsymbol{\xi}_z),\\
R_5 &= (\boldsymbol{\eta}_s, \boldsymbol{\xi}_z) - (\boldsymbol{\eta}_z, \boldsymbol{\xi}_s) - (\tilde{e_c}q, \xi_c),
\end{aligned}$$

with $\Gamma_e = \Gamma_0 \cup \partial\Omega_-$ and $\langle u, v\rangle_e = \int_e uvds$. Now, we estimate $R_i's$ term by term. Using (3.6), hypothesis 1, Lemma 3.2 and the Schwarz inequality, we can get

$$\begin{aligned}
R_1 &\le C\|(\eta_c)_t\|\|\xi_c\| + C\|\boldsymbol{\eta}_s\|\|\boldsymbol{\xi}_s\|\\
&\le Ch^{k+1}\left(\|\xi_c\| + \|\boldsymbol{\xi}_s\|\right),
\end{aligned} \tag{3.18}$$

The estimate of R_2 is slightly complicated,

$$\begin{aligned}
R_2 &\le C\|\mathbf{D}(\mathbf{u}) - \mathbf{D}(\mathbf{u}_h)\|\|\boldsymbol{\xi}_s\|\\
&\le C\|\mathbf{u} - \mathbf{u}_h\|\|\boldsymbol{\xi}_s\|\\
&\le C\left(h^{k+1} + \|\boldsymbol{\xi}_u\|\right)\|\boldsymbol{\xi}_s\|,
\end{aligned} \tag{3.19}$$

where in the first step we use Schwarz inequality and hypothesis 4, the second step follows from Lemma 2.1, and the last step requires Lemma 3.2. We estimate R_3 by dividing it into three parts

$$R_3 = R_{31} + R_{32} + R_{33}, \tag{3.20}$$

where

$$R_{31} = (\mathbf{u}c - \mathbf{u}c_h, \nabla\xi_c) + (\mathbf{u}c_h - \mathbf{u}_h c_h, \nabla\xi_c), \tag{3.21}$$

$$R_{32} = \frac{1}{2}\sum_{e\in\Gamma_e}\langle(2\mathbf{u}c - \mathbf{u}_h^+ c_h^+ - \mathbf{u}_h^- c_h^-)\cdot\boldsymbol{\nu}_e, [\xi_c]\rangle_e, \tag{3.22}$$

$$R_{33} = \frac{1}{2}\sum_{e\in\Gamma_e}\langle\alpha[\eta_c - \xi_c], [\xi_c]\rangle_e. \tag{3.23}$$

Using hypothesis 4 and (3.5), we have

$$\begin{aligned} R_{31} &\le C\left(\|c-c_h\|+\|\mathbf{u}-\mathbf{u}_h\|\right)\|\nabla\xi_c\| \\ &\le C\left(h^{k+1}+\|\boldsymbol{\xi}_u\|+\|\xi_c\|\right)\left(\|\boldsymbol{\xi}_s\|+h^{k+1}\right), \end{aligned} \tag{3.24}$$

where in the first step, we use Schwarz inequality while the second step follows from Lemmas 3.2 and 3.4. The estimate of R_{32} also requires hypothesis 4 and (3.5),

$$\begin{aligned} R_{32} &= \frac{1}{2}\sum_{e\in\Gamma_e}\langle\left(\mathbf{u}(c-c_h^+)+(\mathbf{u}-\mathbf{u}_h^+)c_h^+ + \mathbf{u}(c-c_h^-)+(\mathbf{u}-\mathbf{u}_h^-)c_h^-\right)\cdot\boldsymbol{\nu}_e, [\xi_c]\rangle_e \\ &\le C\left(\|c-c_h\|_{\Gamma_h}+\|\mathbf{u}-\mathbf{u}_h\|_{\Gamma_h}\right)\|[\xi_c]\|_{\Gamma_h} \\ &\le Ch^{\frac{1}{2}}(\|\eta_c\|_{\Gamma_h}+\|\xi_c\|_{\Gamma_h}+\|\boldsymbol{\eta}_u\|_{\Gamma_h}+\|\boldsymbol{\xi}_u\|_{\Gamma_h})\left(\|\boldsymbol{\xi}_s\|+h^{k+1}\right) \\ &\le C\left(h^{k+1}+\|\boldsymbol{\xi}_u\|+\|\xi_c\|\right)\left(\|\boldsymbol{\xi}_s\|+h^{k+1}\right), \end{aligned} \tag{3.25}$$

where in the second step we use Schwarz inequality, the third step follows from Lemma 3.4, the last one requires Lemmas 3.1 and 3.2. Now we proceed to the estimate of R_{33},

$$\begin{aligned} R_{33} &\le C(\|\eta_c\|_{\Gamma_h}+\|\xi_c\|_{\Gamma_h})\|[\xi_c]\|_{\Gamma_h} \\ &\le Ch^{\frac{1}{2}}(\|\eta_c\|_{\Gamma_h}+\|\xi_c\|_{\Gamma_h})(\|\boldsymbol{\xi}_s\|+h^{k+1}) \\ &\le C\left(h^{k+1}+\|\xi_c\|\right)\left(\|\boldsymbol{\xi}_s\|+h^{k+1}\right), \end{aligned} \tag{3.26}$$

where the first step follows from Schwarz inequality, the second step is based on Lemma 3.4, the third one requires Lemma 3.2. Plug (3.24), (3.25) and (3.26) into (3.20) to obtain

$$R_3 \le C\left(h^{k+1}+\|\boldsymbol{\xi}_u\|+\|\xi_c\|\right)\left(\|\boldsymbol{\xi}_s\|+h^{k+1}\right). \tag{3.27}$$

The estimate of R_4 follows from Lemma 3.3

$$R_4 \le Ch^{k+1}\|c\|_{k+2}\|\boldsymbol{\xi}_z\|. \tag{3.28}$$

Now we begin to deal with R_5. Using Lemma 3.2 and the Schwartz inequality, we easily obtain

$$\begin{aligned} R_5 &\le \|\boldsymbol{\eta}_s\|\|\boldsymbol{\xi}_z\|+\|\boldsymbol{\eta}_z\|\|\boldsymbol{\xi}_s\|+C\|\tilde{e_c}\|\|\xi_c\| \\ &\le Ch^{k+1}\left(\|\boldsymbol{\xi}_z\|+\|\boldsymbol{\xi}_s\|\right)+Ch^{k+1}\|\xi_c\|+C\|\xi_c\|^2. \end{aligned} \tag{3.29}$$

Substituting the estimation (3.18), (3.19), (3.27), (3.28), (3.29) into (3.17) and use hypothesis 3, we obtain

$$\begin{aligned} &\frac{d}{dt}\|\phi^{\frac{1}{2}}\xi_c\|^2+\|\boldsymbol{\xi}_s\|^2 \\ \le\ & C\left[\left(h^{k+1}+\|\boldsymbol{\xi}_u\|+\|\xi_c\|\right)\left(\|\boldsymbol{\xi}_s\|+h^{k+1}\right)+h^{k+1}\|\boldsymbol{\xi}_z\|+h^{2(k+1)}+\|\xi_c\|^2\right] \end{aligned} \tag{3.30}$$

Now, we proceed to eliminate $\|\boldsymbol{\xi}_z\|$ on the right-hand side of the above equation. Setting $\boldsymbol{\psi} = \boldsymbol{\xi}_z$ in (3.9) to obtain

$$\begin{aligned}(\boldsymbol{\xi}_z, \boldsymbol{\xi}_z) &= (\boldsymbol{\eta}_z, \boldsymbol{\xi}_z) - (\mathbf{D}(\mathbf{u})\mathbf{s} - \mathbf{D}(\mathbf{u}_h)\mathbf{s}_h, \boldsymbol{\xi}_z) \\ &= (\boldsymbol{\eta}_z, \boldsymbol{\xi}_z) - ((\mathbf{D}(\mathbf{u}) - \mathbf{D}(\mathbf{u}_h))\mathbf{s}, \boldsymbol{\xi}_z) - (\mathbf{D}(\mathbf{u}_h)(\mathbf{s} - \mathbf{s}_h), \boldsymbol{\xi}_z).\end{aligned}$$

Then we have

$$\begin{aligned}\|\boldsymbol{\xi}_z\|^2 &\le \|\boldsymbol{\eta}_z\|\|\boldsymbol{\xi}_z\| + C\|\mathbf{D}(\mathbf{u}) - \mathbf{D}(\mathbf{u}_h)\|\|\boldsymbol{\xi}_z\| + C\left(\|\boldsymbol{\eta}_s\| + \|\boldsymbol{\xi}_s\|\right)\|\boldsymbol{\xi}_z\| \\ &\le Ch^{k+1}\|\boldsymbol{\xi}_z\| + C\|\mathbf{u} - \mathbf{u}_h\|\|\boldsymbol{\xi}_z\| + C\left(h^{k+1} + \|\boldsymbol{\xi}_s\|\right)\|\boldsymbol{\xi}_z\| \\ &\le C\left(h^{k+1} + \|\boldsymbol{\xi}_u\| + \|\boldsymbol{\xi}_s\|\right)\|\boldsymbol{\xi}_z\|,\end{aligned}$$

where in the first step we use (3.6), Schwarz inequality and hypothesis 4, the second step follows from Lemmas 2.1 and 3.2, and the last one requires Lemma 3.2. We can cancel $\|\boldsymbol{\xi}_z\|$ in the above equation to obtain

$$\|\boldsymbol{\xi}_z\| \le C\|\boldsymbol{\xi}_u\| + C\|\boldsymbol{\xi}_s\| + Ch^{k+1} \tag{3.31}$$

Combining (3.30) and (3.31), we have

$$\frac{d}{dt}\|\phi^{\frac{1}{2}}\xi_c\|^2 + \|\boldsymbol{\xi}_s\|^2 \le C\left[\left(h^{k+1} + \|\boldsymbol{\xi}_u\| + \|\xi_c\|\right)\left(\|\boldsymbol{\xi}_s\| + h^{k+1}\right) + \|\xi_c\|^2\right], \tag{3.32}$$

which further yields

$$\frac{d}{dt}\|\phi^{\frac{1}{2}}\xi_c\|^2 + \|\boldsymbol{\xi}_s\|^2 \le C\left(h^{2(k+1)} + \|\boldsymbol{\xi}_u\|^2 + \|\xi_c\|^2\right),$$

Integrate the equation with respect to time between 0 and t to yield the second energy estimate

$$\|\xi_c\|^2 + \int_0^t \|\boldsymbol{\xi}_s\|^2 dt \le C\int_0^t (\|\xi_c\|^2 + \|\boldsymbol{\xi}_u\|^2)dt + Ch^{2(k+1)}. \tag{3.33}$$

Remark 3.1 *To obtain* (3.32)*, we need* $\mathbf{D}$ *to be positive definite, see* (3.17)*. If we assume* $\mathbf{D}$ *to be positive semidefinite, then the* $\|\xi_s\|$ *term on the right-hand side of* (3.32) *cannot be eliminated.*

3.6 Proof of the error estimate

Now we are ready to combine the two energy inequalities to finish the proof of Theorem 2.1. Firstly, combing (3.16) with (3.33), we obtain

$$\|\xi_c\|^2 + \int_0^t \|\boldsymbol{\xi}_s\|^2 dt \le C\int_0^t \|\xi_c\|^2 dt + Ch^{2(k+1)}. \tag{3.34}$$

Employing Gronwall's inequality, we have

$$\|\xi_c\|^2 + \int_0^T \|\boldsymbol{\xi}_s\|^2 dt \leq Ch^{2(k+1)}.$$

which further yield

$$\|\boldsymbol{\xi}_u\| \leq Ch^{k+1}$$

by the first energy estimate (3.16). Finally, by using the standard approximation result, we obtain (2.17). To complete the proof, let us verify the a priori assumption (3.4). For $k \geq 1$, we can consider h small enough so that $Ch^{k+1} < \frac{1}{2}h$, where C is the constant determined by the final time T. Then if $t^* = \inf\{t : \|c - c_h\| + \|\mathbf{u} - \mathbf{u}_h\| \geq h\}$, we should have $\|c - c_h\| + \|\mathbf{u} - \mathbf{u}_h\| = h$ by continuity in time at $t = t^*$. However, if $t^* < T$, theorem 2.1 implies that $\|c - c_h\| + \|\mathbf{u} - \mathbf{u}_h\| \leq Ch^{k+1}$ for $t \leq t^*$, in particular $h = \|(c - c_h)(t^*)\| + \|(\mathbf{u} - \mathbf{u}_h)(t^*)\| \leq Ch^{k+1} < \frac{1}{2}h$, which is a contradiction. Therefore, there always holds $t^* \geq T$, and thus the a priori assumption (3.4) is justified.

4 Numerical experiments

In this section, we provide numerical examples to illustrate the accuracy and capability of the method. Time discretization is given as the third order strong-stability-preserving Runge-Kutta method [26]. We take the time step to be sufficiently small such that the error in time is negligible compared to spatial error. In the scheme, the numerical flux in the convection term is taken as $\widehat{\mathbf{u}_h c_h} = \frac{1}{2}(\mathbf{u}_h^+ c_h^+ + \mathbf{u}_h^- c_h^-)$. We simulate the problem on the computational domain $\Omega = [0,1]\times[0,1]$ up to $T = 0.01$ with time step is $\Delta t = r * h^2$, where r varies based on the polynomial degrees. In all the following experiments, if not otherwise stated, we take $\kappa(x, y) = 1$, $\mu(c) = 1$ and use uniform meshes with $N_x = N_y = N = 100$.

Example 4.1 *We first consider the problem with matrix* $\mathbf{D}(\mathbf{u}) = \gamma\mathbf{I}$*, where* γ *is a constant. In addition, we take the initial condition* $c_0 = sin(2\pi(x + y))$*,* $\phi(x, y) = 1$ *and add a source*

$$f = 2\pi cos(2\pi(x + y + t))(4\pi(x + y + t) + 1) + 8\gamma\pi^2 sin(2\pi(x + y + t))$$

in the concentration equation.

The exact solution is

$$c = \sin(2\pi(x + y + t)), \quad \mathbf{u} = (4\pi x + 2\pi t, 4\pi y + 2\pi t).$$

The L^2 error with with $\gamma = 1$ and 0.01 are contained in Tables 1 and 2, respectively. We can see that the method with Q^k elements gives a $(k + 1)-$th order of accuracy in L^2 norm.

Table 1: The numerical results for c with $\gamma = 1$.

N	$Q^1/r = 0.01$		$Q^2/r = 0.01$		$Q^3/r = 0.001$	
	L^2 error	order	L^2 error	order	L^2 error	order
10	2.3022e-02	–	7.9943e-04	–	2.7981e-04	–
20	5.7645e-03	2.00	9.9829e-05	3.00	1.7493e-05	4.00
40	1.4416e-03	2.00	1.2511e-05	3.00	1.0965e-06	4.00
80	3.5950e-04	2.00	1.5632e-06	3.00	6.8294e-08	4.00
160	9.0167e-05	2.00	1.9586e-07	3.00	4.2649e-09	4.00

Table 2: The numerical results for c with $\gamma = 0.01$.

N	$Q^1/r = 0.01$		$Q^2/r = 0.01$		$Q^3/r = 0.001$	
	L^2 error	order	L^2 error	order	L^2 error	order
10	2.3022e-02	–	7.9894e-04	–	2.7991e-04	–
20	5.7503e-03	2.00	9.9566e-05	3.00	1.7474e-05	4.00
40	1.4420e-03	2.00	1.2450e-05	3.00	1.0895e-06	4.00
80	3.5982e-04	2.00	1.5557e-06	3.00	6.8323e-08	4.00
160	9.0254e-05	2.00	1.9480e-07	3.00	4.2650e-09	4.00

Example 4.2 *We consider the problem with matrix* $\mathbf{D}(\mathbf{u}) = \mathbf{u} \otimes \mathbf{u} + I$. *In addition, we choose the initial condition* $c_0 = sin(2\pi(x + y))$, *and add a source*

$$f = 2\pi cos(2\pi(x+y+t))(4\pi(x+y+t))(1-12\pi^2)+4\pi^2(16\pi^2(x+y+t)^2+2)sin(2\pi(x+y+t))$$

in the concentration equation.

The exact solution is

$$c = \sin(2\pi(x + y + t)), \quad \mathbf{u} = (4\pi x + 2\pi t, 4\pi y + 2\pi t).$$

The L^2 errors and the numerical orders of accuracy at time $t = 0.01$ and $t = 1$ with uniform meshes is contained in Tables 3. We can see that the method with Q^k elements also gives a $(k + 1)-$th order of accuracy in L^2 norm.

Example 4.3 *Now we take the porosity* $\phi = 0.1$, *the tensor* $\mathbf{D} = diag\{1, 1\}$. *We choose the initial condition* $c_0 = sin(\pi x) * sin(\pi y)$. *We consider a production well located in the computational domain. The sink* q *and the velocity field* $\mathbf{u}$ *are taken as*

$$q = -2\pi^2 \sin(\pi x) \sin(\pi y), \quad \mathbf{u} = (\pi \cos(\pi x) \sin(\pi y), \pi \sin(\pi x) \cos(\pi y))^T,$$

respectively.

Table 3: The numerical results for c.

t	N	$Q1/r = 0.01$		$Q2/r = 0.01$		$Q3/r = 0.001$	
		L^2 error	order	L^2 error	order	L^2 error	order
0.01	10	2.5639E-02	–	8.4515E-04	–	6.2181E-04	–
	20	6.4217E-03	2.00	1.0544E-04	3.00	3.8917E-05	4.00
	40	1.6090e-03	2.00	1.3178e-05	3.00	2.4310e-06	4.00
	80	4.0142e-04	2.00	1.6480e-06	3.00	1.5222e-07	4.00
	160	1.0018e-04	2.00	2.0601e-07	3.00	9.4942e-08	4.00
1	10	8.1619e-02	–	8.0873e-04	–	4.6787e-04	–
	20	2.0505e-02	1.99	1.0119e-05	3.00	2.9266e-05	4.00
	40	5.1511e-03	1.99	1.2736e-05	2.99	1.8293e-06	4.00
	80	1.2873e-03	2.00	1.5825e-06	3.00	1.1432e-07	4.00
	160	3.1982e-04	2.00	1.9743e-07	3.00	7.1342e-09	4.00

The velocity field $\mathbf{u}$ and initial concentration are shown in Figure 1, and the concentration at $\frac{T}{4}$, $\frac{T}{2}$, $\frac{3T}{4}$ and T are shown in Figure 2. From Figure 2, we can easily observe that the total mass of c is decreasing, and the fluid mixture is getting out of the production well.

Example 4.4 *We change the initial condition in Example 4.3 to*

$$c_0 = \begin{cases} 0.001, & (x-0.5)^2 + (y-0.5)^2 < 0.09, \\ 0, & \textit{otherwise}, \end{cases}$$

and the velocity field $\mathbf{u} = (0.1, 0.4)$ *is a constant vector. Therefore, the source* $q = 0$*, i.e. no injection or production wells exist in the computational domain.*

The velocity field $\mathbf{u}$ and initial concentration are given in Figure 3. Moreover, we also plot the concentrations at $\frac{T}{3}$, $\frac{2T}{3}$ and T in Figure 4. In this problem, the total mass $\int_\Omega c dV$ is a constant during the time evolution. We numerically monitor the total mass which is equal to $9\pi \times 10^{-5}$ for all t.

5 Concluding remarks

In this paper, we apply LDG methods to flow and transport equations in 2-dimensional coupled system of incompressible miscible displacement problem. The optimal order of error estimate holds for the solution itself and also for some auxiliary variables for incompressible miscible displacement problem under suitable norms. Special projections and a priori assumption help to eliminate the jump terms at the cell boundaries and provide the boundedness of the numerical approximations. In general, it is not easy to apply this method to the models with positive semi-definite $\mathbf{D}(\mathbf{u})$, we will continue this work in the

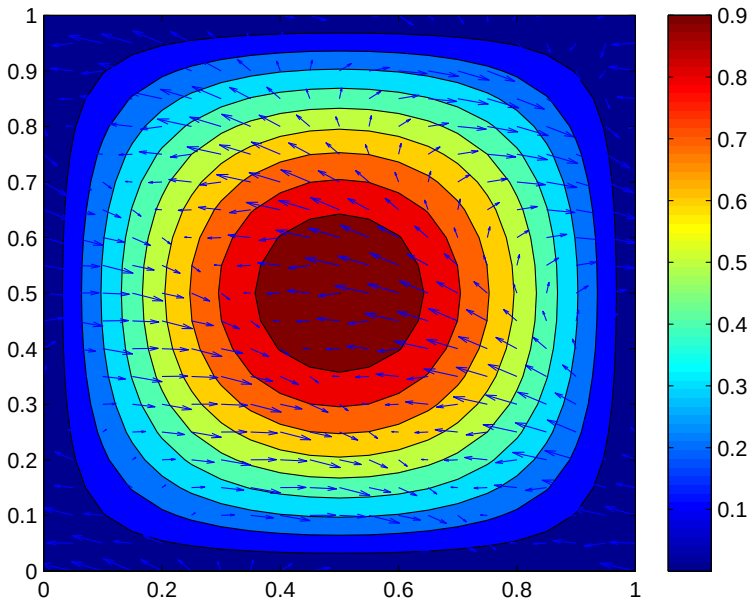

Figure 1: The velocity field and initial concentration in Example 4.3.

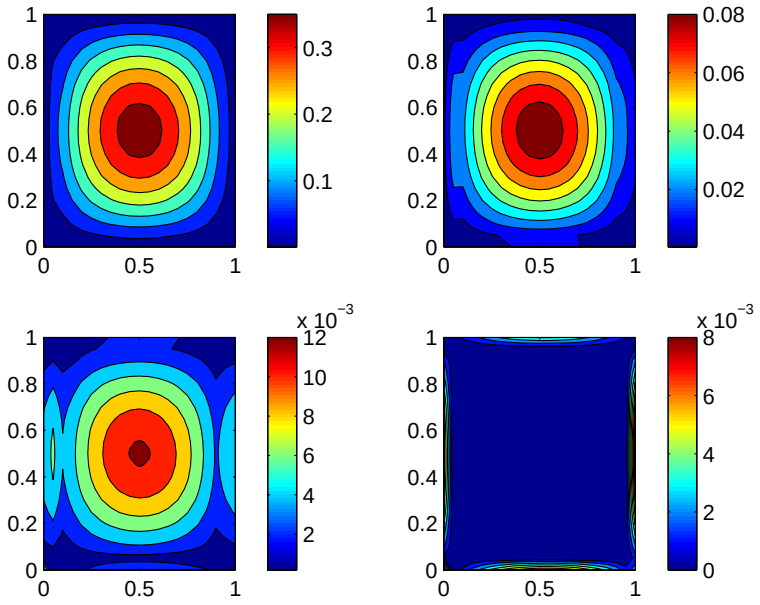

Figure 2: The concentrations c at $\frac{T}{4}$ (top left), $\frac{T}{2}$ (top right), $\frac{3T}{4}$ (bottom left) and T (bottom right) in Example 4.3.

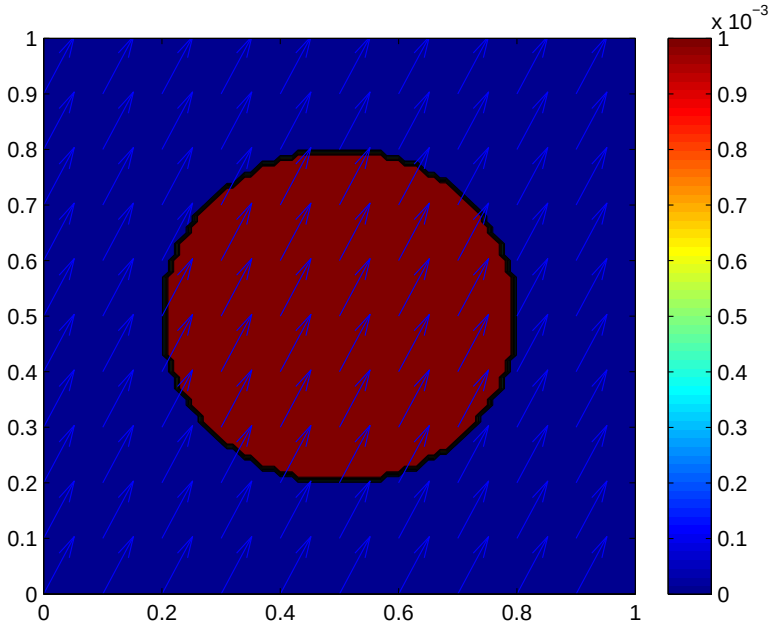

Figure 3: The velocity field and initial concentration in Example 4.4.

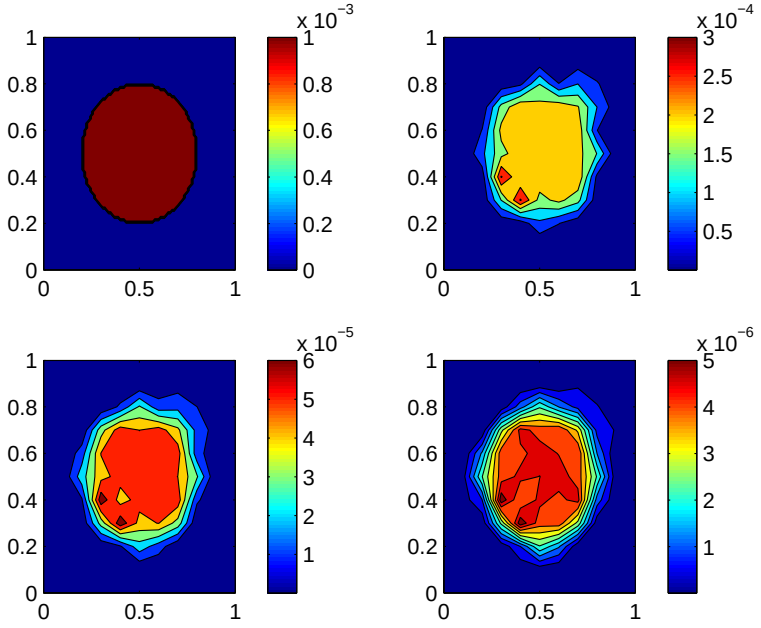

Figure 4: The concentrations c at 0 (top left), $\frac{T}{3}$ (top right), $\frac{2T}{3}$ (bottom left) and T (bottom right) in Example 4.4.

future. Other possible future works include the study for P^k polynomials instead of Q^k ones.

Acknowledgments

This work was supported by National Natural Science Foundation of China(11571367) and the Fundamental Research Funds for the Central Universities. The author would like to express sincere thanks to the referees for valuable comments and suggestions.

Reference

[1] B. Amaziane and M. Ossmani, *Convergence analysis of an approximation to miscible fluid flows in porous media by combining mixed finite element and finite volume methods,* Numerical Methods for Partial Differential Equations, 24 (2007), 799-832.

[2] S. Bartels, M. Jensen and R. Müller, *Discontinuous Galerkin finite element convergence for incompressible miscible displacement problem of low regularity,* SIAM Journal on Numerical Analysis, 47 (2009), 3720-3743.

[3] F. Bassi and S. Rebay *A high-order accurate discontinuous finite element method for the numerical solution of the compressible Navier-Stokes equations,* Journal of Computational Physics, 131 (1997), 267-279.

[4] J. Bear, *Dynamics of fluids in porous media,* Dover Publications, Inc, New York, 764, 1972.

[5] B. Cockburn, G. Kanschat, I. Perugia and D. Schötzau, *Superconvergence of the local discontinuous Galerkin method for elliptic problems on cartesian grids,,* SIAM Journal on Numerical Analysis, 39 (2001), 264-285.

[6] C. Chainais-Hillairet, S. Krell, A. Mouton, *Convergence analysis of a DDFV scheme for a system describing miscible fluid flows in porous media,* Numerical Methods for Partial Differential Equations, 31 (2015), 723-760.

[7] P. Ciarlet, *The finite element method for elliptic problem,* North Holland, 1975.

[8] B. Cockburn *An introduction to the Discontinuous Galerkin method for convection-dominated problems,* Advanced Numerical Approximation of Nonlinear Hyperbolic Equations, volume 1697 of the series Lecture Notes in Mathematics, 150-268, 2006.

[9] B. Cockburn and C.-W. Shu, *The local discontinuous Galerkin method for time-dependent convection-diffusion systems,* SIAM Journal on Numerical Analysis, 35 (1998), 2440-2463.

[10] M. Cui, *Analysis of a semidiscrete discontinuous Galerkin scheme for compressible miscible displacement problem,* Journal of Computational and Applied Mathematics, 214 (2008), 617-636.

[11] J. Douglas, Jr., R.E. Ewing and M.F. Wheeler, *A time-discretization procedure for a mixed finite element approximation of miscible displacement in porous media,* R.A.I.R.O. Analyse numérique, 17 (1983), 249-256.

[12] J. Douglas, Jr., R.E. Ewing and M.F. Wheeler, *The approximation of the pressure by a mixed method in the simulation of miscible displacement,* R.A.I.R.O. Analyse numérique, 17 (1983), 17-33.

[13] F. Dullien, *Porous media fluid transport and pore structure,* Academic press, Inc, New York, 1979

[14] R. E. Ewing and T. F. Russell, *Efficient time-stepping methods for miscible displacement problems in porous media,* SIAM Journal on Numerical Analysis, 19 (1982), 1-67.

[15] R.E. Ewing, T.F. Russell and M.F. Wheeler, *Convergence analysis of an approximation of miscible displacement in porous media by mixed finite elements and a modified method of characteristics,* Computer Methods in Applied Mechanics and Engineering, 47 (1984), 73-92.

[16] R. E. Ewing and M. F. Wheeler, *Galerkin methods for miscible displacement problems in porous media,* SIAM Journal on Numerical Analysis, 17 (1980), 351-365.

[17] X. Feng, *Recent developments on modeling and analysis of flow of miscible fluids in porous media,* in Fluid Flow and Transport in Porous Media: Mathematical and Numerical Treatment (South Hadley, MA, 2001), Contemp. Math. 295, AMS, Providence, RI, 2002, 219-240.

[18] I.M. Gelfand, *Some questions of analysis and differential equations*, American Mathematical Society Translations, 26 (1963), 201-219.

[19] H. Guo, Q. Zhang and Y. Yang, *A combined mixed finite element method and local discontinuous Galerkin method for miscible displacement problem in porous media,* Science China Mathematics, 57 (2014), 2301-2320.

[20] A.E. Hurd and D.H. Sattinger, *Questions of existence and uniqueness for hyperbolic equations with discontinuous coefficients*, Transactions of the American Mathematical Society, 132 (1968), 159-174.

[21] J. Jaffre and J.E. Roberts, *Upstream weighting and mixed finite elements in the simulation of miscible displacements,* ESAIM: Mathematical Modelling and Numerical Analysis, 19 (1985), 443-460.

[22] S. Kumar, *A mixed and discontinuous Galerkin finite volume element method for incompressible miscible displacement problems in porous media,* Numerical Methods for Partial Differential Equations, 28 (2012), 1354-1381.

[23] X. Li and H. Rui, *A MCC finite element approximation of incompressible miscible displacement in porous media,* Computers and Mathematics with Applications, 70 (2015), 750-764.

[24] B. Rivière, *Discontinuous Galerkin finite element methods for solving the miscible displacement problem in porous media,* Ph.D. Thesis, The University of Texas at Austin, 2000.

[25] T. F. Russell and M. F. Wheeler, *Finite element and finite difference methods for continuous flows in porous media,* in The Mathematics of Reservoir Simulation, R. E. Ewing, ed., Frontiers Applied Mathematics 1, SIAM, Philadelphia, 1983, 35-106.

[26] C.-W. Shu and S. Osher, *Efficient implementation of essentially non-oscillatory shock-capturing schemes,* Journal of Computational Physics, 77 (1988), 439-471.

[27] S. Sun, B. Rivière and M.F. Wheeler, *A combined mixed finite element and discontinuous Galerkin method for miscible displacement problem in porous media,* Recent Progress in Computational and Applied PDEs, Tony Chan et al. (Eds.), Kluwer Academic Publishers, Plenum Press, Dordrecht, NewYork, 2002, 323-351.

[28] S. Sun and M.F. Wheeler, *Discontinuous Galerkin methods for coupled flow and reactive transport problems,* Applied Numerical Mathematics, 52 (2005), 273-298.

[29] H. Wang, D. Liang, R. E. Ewing, S. L. Lyons, and G. Qin, *An approximation to miscible fluid flows in porous media with point sources and sinks by an Eulerian-Lagrangian localized adjoint method and mixed finite element methods,* SIAM Journal on Scentific Computing, 22 (2000), 561-581.

[30] H. Wang, C.-W. Shu and Q. Zhang, *Stability and error estimates of local discontinuous Galerkin methods with implicit-explicit time-marching for advection-diffusion problems,* SIAM Journal on Numerical Analysis, 53 (2015), 206-227.

[31] H. Wang, C.-W. Shu and Q. Zhang, *Stability analysis and error estimates of local discontinuous Galerkin methods with implicit-explicit time-marching for nonlinear convection-diffusion problems,* Applied Mathematics and Computation, 272 (2016), 237-258.

[32] H. Wang, S. Wang, Q. Zhang and C.-W. Shu, *Local discontinuous Galerkin methods with implicit-explicit time-marching for multi-dimensional convection-diffusion problems,* ESAIM: M2AN, 50 (2016), 1083-1105.

[33] Y. Wei, *Stabilized finite element methods for miscible displacement in porous media,* ESAIM: Mathematical Modelling and Numerical Analysis, 28 (1994), 611-665.

[34] M. F. Wheeler and B. L. Darlow, *Interiori penalty Galerkin methods for miscible displacement problems in porous media,* Computational Methods in Nonlinear Mechanics, North-Holland, Amsterdam, 1980, 458-506.

[35] Y. Xu and C.-W. Shu, *Local discontinuous Galerkin methods for nonlinear Schrödinger equations,* Journal of Computational Physics, 205 (2005), 72-97.

[36] Y. Xu and C.-W. Shu, *Local discontinuous Galerkin methods for the Kuramoto-Sivashinsky equations and the Ito-type coupled KdV equations,* Computer Methods in Applied Mechanics and Engineering, 195 (2006), 3430-3447.

[37] J. Yan and C.-W. Shu, *A local discontinuous Galerkin method for KdV type equations,* SIAM Journal on Numerical Analysis, 40 (2002), 769-791.

[38] D. Yang, *Mixed methods with dynamic finite-element spaces for miscible displacement in porous media,* Journal of Computational and Applied Mathematics, 30 (1990), 313-328.

[39] Y. Yang and C.-W. Shu, *Analysis of optimal superconvergence of local discontinuous Galerkin method for one-dimensional linear parabolic equations,* Journal of Computational Mathematics, 33 (2015), 323-340.

[40] Y. Yuan, *Characteristic finite element methods for positive semidefinite problem of two phase miscible flow in three dimensions,* Chinese Science Bulletin, 22 (1996), 2027-2032.

[41] Q. Zhang and C.-W. Shu, *Error estimates to smooth solutions of Runge-Kutta discontinuous Galerkin methods for scalar conservation laws*, SIAM Journal on Numerical Analysis, 42 (2004), 641-666.

[42] Q. Zhang and C.-W. Shu, *Stability analysis and a priori error estimates to the third order explicit Runge-Kutta discontinuous Galerkin method for scalar conservation laws*, SIAM Journal on Numerical Analysis, 48 (2010), 1038-1063.